A Two-Stage Color Correction Algorithm for Facial Image

Huilin Liu [a], Lijuan Wang [b], Peng Qian [a], Ying Xu [b], Zhumei Sun [a], Chunrong Guo [a] and Fufeng Li [b*]

[a] *Basic Medical College, Shanghai University of Traditional Chinese Medicine, 1200 Cailun Road, Shanghai, 201203, China.*
[b] *Laboratory of TCM Four Processing, Shanghai University of Traditional Chinese Medicine, 1200 Cailun Road, Shanghai, 201203, China.*

Original Research Article

ABSTRACT

Aims: Facial image analysis is the main direction of facial diagnosis objectification, where realistic colors in medical facial images are essential clues for disease diagnosis. However, the same person's facial color information will have different display information under different light sources and display devices, which may lead to different diagnostic results.
Methodology: Firstly, we conducted group experiments on the selection of color patches and selected 12 face-related color patches for color correction of facial images. Next, to adapt to this task under different lighting conditions, we utilize an adaptive white balance algorithm to adjust brightness as the first step. We selected the D65 illuminate environment as the standard lighting condition. Finally, we employed a polynomial-regression algorithm based on ridge regression for color correction.
Results: The experimental results demonstrate that the average values of the chromatic distance of our method under all five lighting conditions are less than 3.0. We also compare the ablation experiments of adjusting brightness.

Corresponding author: E-mail: li_fufeng@aliyun.com;

Conclusion: The results indicate that the proposed method has good consistency in color correction of facial images under different lighting conditions, which is more suitable for clinical medical diagnosis.

1. INTRODUCTION

With the continuous development of artificial intelligence technology, researchers have increasingly used computer-aided diagnosis in the field of clinical diagnosis. In traditional Chinese medicine (TCM), facial color inspection is an important diagnostic method that conveys abundant valuable information about patients' physiological conditions and pathological changes [1]. However, even for the same face, the captured facial images taken by different cameras under different lighting conditions display different color appearances on the monitor [2]. It may lead to different diagnosis results by clinical doctors and thus harm patients' health. Therefore, color correction of facial images is essential for computer-aided image analysis of clinical diagnosis.

Many scientific researchers apply digital image technology to realize the potential of color correction in medical diagnosis. In the process of research, lots of methods have been investigated, such as polynomial(POLY)-based methods [3-5], support vector regression (SVR)-based methods [6-8], and neural network-based methods [2,9,10]. The most common color correction method is to calculate the mapping relationship between the correct color space and the target color space. Finlayson et al. [3] used an alternating least squares algorithm for nonuniform intensity color correction in the 24-patch Macbeth color checker. Graham et al. [4] applied root-polynomial regression to enhance color correction performance on real and synthetic data. Zhang et al. [5] employed a polynomial transform-based correction algorithm to portray the facial images and facilitate quantitative analysis before feature extraction and classification. Besides, Zhuo et al. [6] designed a K-PLSR method for color correction under different lighting conditions. Bo et al. [7] introduced SVR to reproduce the colors of the nonlinear imaging system.

On the other hand, many researchers have exploited many image data and neural network-based correction methods to achieve the effectiveness of feature extraction. Zhou et al. [9] employed an SA-GA-BP network for TCM image

color correction. They selected color patches that are similar to the tongue and skin to reduce the complexity of training processing. Zhang et al. [10] designed a MEC-BP-Adaboost for color image correction. Lu et al. [2] utilized an improved convolutional neural network (CNN) and synthesized about 2000 images as a training set to adapt to different work environments for color appearance. However, obtaining many facial images is difficult because of marking costs and patient privacy. If a large number of training samples is lacking, this algorithm is unsuitable for facial image correction [11].

Images captured under different lighting conditions will have different visual appearances depending on the illumination and color temperature. According to the International Commission on Illumination (CIE) recommendations, a D65 light source with a color temperature of 6500K can be selected as the standard lighting environment to simulate daylight [2]. Therefore, some scholars carried out image color correction tasks for color deviation under different lighting conditions. Akazawa et al. [12] proposed a three-color balance adjustment for color constancy correction. Yan et al. [13] designed an adaptive white balance method by statistical prior to mitigate the impact of color deviation. Huang et al. [14] employed a white balance conversion method with Digital SG ColorChecker for color correction.

Motivated by the functional gaps in current facial color correction in the case of small samples, we proposed two-stage color correction for face color correction. The patient is generally required to be photographed under a standard light condition, but it is challenging to meet the condition in the natural environment. Due to the influence of various lighting conditions, the color appearance of facial images varies over a wide range. The proposed method applies an adaptive white-balanced algorithm, as the first stage, to adjust the brightness of the facial image. Then, it utilizes a polynomial-based method to learn the color mapping model between the distorted and target color images for color correction. Besides, this method can be applied to small sample datasets.

This study demonstrates three aspects as follows:

1. Instead of using a single correction method, we combined a white-balanced algorithm and a polynomial-based method for color correction under different illuminate environments.
2. We tested group experiments on selecting color patches in 24 Xrite ColorChecker and selected 12 face-related color patches for color correction.
3. Experiments conducted that the proposed method performs well for color correction tasks under five different lighting conditions.

The remainder of this paper is organized as follows. Details of the proposed method are described in Section 2. The experimental results are analyzed in Section 3. The discussion is presented in Section 4. Finally, conclusions and future work are summarized in Section 5.

2. METHODOLOGY

2.1 Overview

This section demonstrates the proposed correction algorithm for medical facial images, illustrated in Fig. 1. The input is a distorted image containing face and color patches. Firstly, the distorted image is adjusted overall brightness by the proposed adaptive white-balance-based algorithm. Next, the color space values are extracted from the processed image, and the facial image is identified using 68-point face detection [15] and cropped. Then, the color correction algorithm is used to optimize the mapping relationship between the distorted and target D65 color space values. Finally, the facial image is input into the optimized color correction model to obtain the corrected image.

The dataset of the images in this study was 24-bit images of the face, including some background information, with a spatial resolution of 3840×2880 pixels, collected from the digital laboratory of four diagnoses of TCM, Shanghai University of Traditional Chinese Medicine, Shanghai, China. The volunteers are selected from the Shanghai University of Traditional Chinese Medicine students. Informed consent to publish identifying images has been obtained. The facial images were captured by specialized equipment under five different lighting conditions. The equipment includes two assisted light sources and a portable camera with photographing medium (see Fig. 2). The photograph takes a distance of 23cm-26cm between the camera and the face. These lighting conditions include D50 illumination (1337lx, 5186k), D65 illumination (1830lx, 6991k), D65 illumination with warm light (5023lx, 5171k), warm light (3751lx, 4231k), and weak light (5lx, 5617k), and each lighting condition contains 50, 46, 45, 47, and 40 images, respectively. Besides, each captured image contains a face and a color checker.

We selected the D65 color checker for facial color correction as the target lighting environment. Considering the shooting angle under different lighting conditions, the color card data taken each time is slightly different. To avoid enlarging the difference in D65 standard color card values, we selected the average value of color cards collected under the D65 lighting condition as reference data.

2.2 Color Patch Selection

All 24 color patches are selected from color reference as training samples for the facial colour correction task, increasing the complexity of models [1]. In addition, some colors of color patches in the ColorChecker (Fig. 3) are unlikely to appear in the facial images. Inspired by the color patch selection method of Ref [16], we conducted group experiments on the selection of color patches in Xrite ColorChecker as shown below:

1. Group A: 8 basic skin-related color patches (numbered from 1 to 8): six different levels of grayscale patches and two skin color patches.
2. Group B: 12 face-related color patches (numbered from 1 to 12): six different levels of grayscale patches, four red-related color patches, and two skin color patches.
3. Group C: 24 standard color patches.

2.3 Brightness Adjustment

The captured images under different lighting conditions will display different color information on the monitor. Therefore, we apply a white-balance-based algorithm [17] to detect and adjust the overall brightness of the captured images. The improved algorithm adjusts the overall color of white objects in the image according to their color drift. Since it is difficult to have pure white objects in facial images, the algorithm uses the color value of the white patch (No.6 patch in Fig. 3) on the target color checker as the reference white pixels instead of using the highest luminance value as the gain of the standard white.
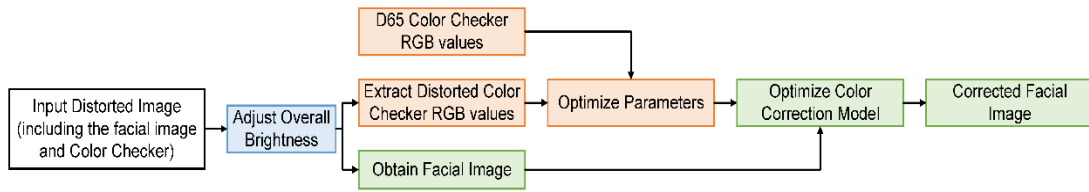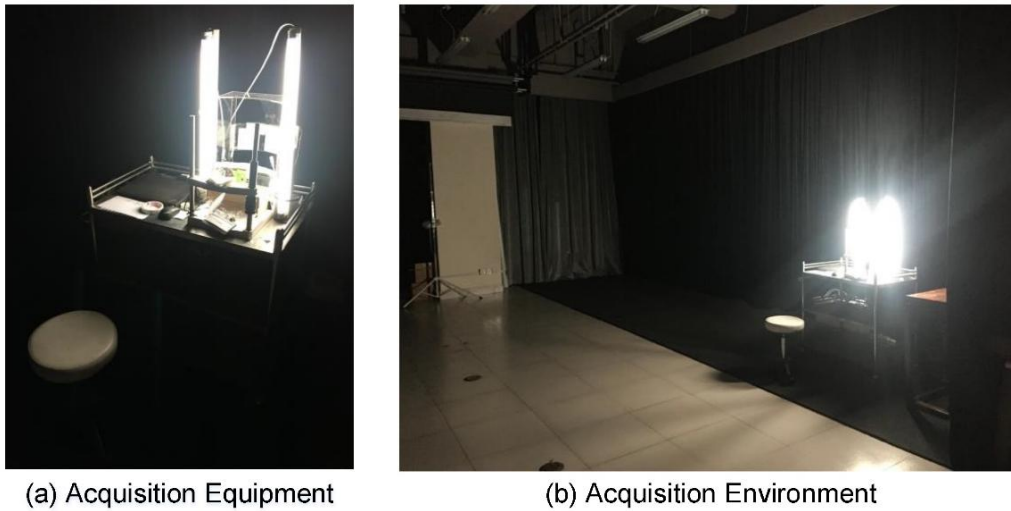
Fig. 1. The pipeline of the proposed correction algorithm

(a) Acquisition Equipment　　　　　(b) Acquisition Environment

Fig. 2. The acquisition device in a dark environment

Fig. 3. 24 Xrite color checker (numbered color patches)

The original RGB value $(R_{org}, G_{org}, B_{org})$ of the input image is obtained in RGB color space. Next, we transfer RGB color space to YCrCb color space and calculate the RGB average value (R_w, G_w, B_w) and the YCrCb average value (Y_w, Cr_w, Cb_w) of the No. 6 color patch in the target color space.

The first scale factor $(R_{scale}, G_{scale}, B_{scale})$ using reference white pixels is done by the following formulas:

$$\begin{cases} R_{scale} = Y_w / R_w \\ G_{scale} = Y_w / G_w \\ B_{scale} = Y_w / B_w \end{cases} \tag{1}$$

Then the second scale factor $(R_{GWA}, G_{GWA}, B_{GWA})$ is

$$\begin{cases} R_{GWA} = Gray / R_{aver} \\ G_{GWA} = Gray / G_{aver} \\ B_{GWA} = Gray / B_{aver} \end{cases} \tag{2}$$

Where $Gray = (R_{aver} + G_{aver} + B_{aver})/3$, and $(R_{aver}, G_{aver}, B_{aver})$ is the average value of $(R_{org}, G_{org}, B_{org})$.

2.4 Correction Regression Algorithm

The color card images captured under different illuminate environments are taken as data samples to obtain target and distorted color values of each color patch. Then, the color correction model learns the mapping relationship between the distorted and target color images.

Suppose the target color checker has N color patches, and these three-channel values of the *i*-th color patch are R_{0i}, G_{0i}, and B_{0i}. The three-channel values of the *i*-th color patch in the distorted color checker are R_i, G_i, and B_i ($i = 1, 2, 3, \ldots, N$). It can be represented as the following formula:

$$\begin{cases} R_{0i} = a_{11}s_{1i} + a_{12}s_{2i} + \ldots + a_{1i}s_{mi} \\ G_{0i} = a_{21}s_{1i} + a_{22}s_{2i} + \ldots + a_{2i}s_{mi} \ (i = 1, 2, \ldots, N) \\ B_{0i} = a_{31}s_{1i} + a_{32}s_{2i} + \ldots + a_{3i}s_{mi} \end{cases} \tag{3}$$

Where $s_{mi} (m = 1, \ldots, M)$ is formed by

polynomials of R_i, G_i, and B_i, and the polynomial terms $M = \left[1, R, G, B, R \times G, R \times B, G \times B, R^2, G^2, B^2 \right]$.

The above system of equations is transferred to the matrix as follows:

$$X = A^T * S \tag{4}$$

Where X is the RGB matrix of a target color card with dimension $3 \times I$, A is the conversion coefficient matrix to be solved with dimension $I \times 3$, and S is the polynomial regression matrix with dimension $M \times I$, respectively expressed as follows.

$$X = \begin{bmatrix} R_{01} & R_{02} & \cdots & R_{0i} \\ G_{01} & G_{02} & \cdots & G_{0i} \\ B_{01} & B_{02} & \cdots & B_{0i} \end{bmatrix}, \quad A = \begin{bmatrix} a_{11} & a_{12} & a_{13} \\ a_{21} & a_{22} & a_{23} \\ \vdots & \vdots & \vdots \\ a_{s1} & a_{s2} & a_{s3} \end{bmatrix},$$

$$S = \begin{bmatrix} s_{11} & s_{12} & s_{13} & & s_{1I} \\ s_{21} & s_{22} & s_{23} & \cdots & s_{2I} \\ s_{31} & s_{32} & s_{33} & & s_{3I} \\ & \vdots & & \ddots & \vdots \\ s_{M1} & s_{M2} & s_{M3} & \cdots & s_{MI} \end{bmatrix}$$

The regression matrix A obtained by the ridge regression algorithm is:

$$A = \left(MM^T + \lambda I \right)^{-1} M X^T \tag{5}$$

Where I is the identity matrix and λ is the adjustment parameter to control the increased penalty force for $\|\beta\|^2$. The increase of λ can reduce the variance of model error and make the generalization ability stronger, but it will increase the deviation of model error. In the experiment, the generalized cross-validation method is employed in the ridge trace map to obtain the adjustment parameter ($\lambda = 0.003$) that minimizes the mean square deviation of the model.

Finally, after obtaining coefficient regression matrix A, the corrected facial image is calculated by the following formulas:

$$X_{output} = A^T * S_{input} \tag{6}$$

Where S_{input} is the cropped image after 68-point face detection, and X_{output} is the RGB matrix of the corrected facial image. Finally, the corrected

458

facial image can be calculated to realize the color correction.

3. RESULTS AND DISCUSSION

3.1 Experimental Settings

Because of visual differences in chromaticity, the evaluation methods of color correction algorithms have two components: objective evaluation and subjective evaluation.

The objective evaluation is to calculate the chromatic distance of color patches. If the chromatic distance $\Box E \geq 3.0$ in the CIE LAB color space, two different visual perceptions will appear. The value is calculated by the following formulas:

$$\Delta E_k = \sqrt{\left(L_{ki} - L_{kj}\right)^2 + \left(a_{ki} - a_{kj}\right)^2 + \left(b_{ki} - b_{kj}\right)^2} \quad (7)$$

Where k represents the k-th color patch, i is the distorted color checker, and j denotes the standard color checker under the D65 lighting condition. ΔE_{mean} is the average of chromatic distances of the color patches.

The subjective evaluation is when a certain number of observers visually evaluate the color quality of the corrected images. From the subjective perception of Fig. 4, the color checkers under different lighting conditions have different visual perceptions. The color checkers after correction are similar to that under the D65 illumination condition.

3.2 RESULTS

3.2.1 Results of baseline method selection

To obtain the evaluation results for the objective analysis, we selected color patches (10×10 pixels) from each color checker to calculate the chromatic distance. We compared POLY-(1), SVR-(11), and CNN-based [18] color correction methods with 24 color patches. We used SVR

(11) and Gaussian kernels to build the mapping relationship. Three parameters need to be optimized, i.e., penalty factor C, the gamma of Gaussian kernel g, and epsilon of lost function p. Eventually, they are set to 20, 0.03, and 0, respectively.

As can be seen from Fig. 5, the ΔE_{mean} of above color correction algorithms based on 24 color patches under five illumination conditions were significantly reduced, and even the ΔE_{mean} of CNN algorithm was below 2. However, the visual comparisons of CNN (see Fig. 5-6) showed significant distortion, demonstrating that CNN was unsuitable for small datasets. Moreover, no significant difference of ΔE_{mean} between uncorrected images and that of SVR was noted. Moreover, the correction results of POLY were better than those of SVR. Therefore, we applied the polynomial regression-based algorithm for subsequent experiments on color patch selection.

3.2.2 Results of color patches selection

According to Section 2.1, we compared the POLY--based algorithm on the above three groups (Group A, Group B, and Group C). In Fig. 7, the values of group A are higher than the color difference before correction. On the contrary, the average difference between groups B and C was similar, and both were lower than the color difference before correction. Fig. 8 shows examples of facial color correction for visual comparison. The figure shows insignificant differences in corrected facial images between groups B and C.

It can be seen that it is not essential to select all color patches (Group C) as training samples to correct facial images. In addition, irrelevant color patches will affect the objective analysis results. Therefore, it is demonstrated that the 12 selected color patches are sufficient for this facial color correction task.
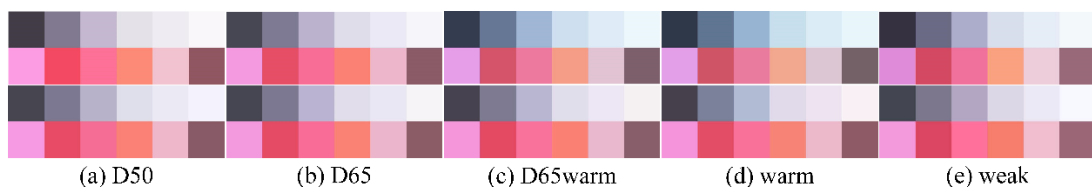

(a) D50   (b) D65   (c) D65warm   (d) warm   (e) weak

Fig. 4. The color checkers under different lighting conditions (upper row) and their corrected results of our method (bottom row)
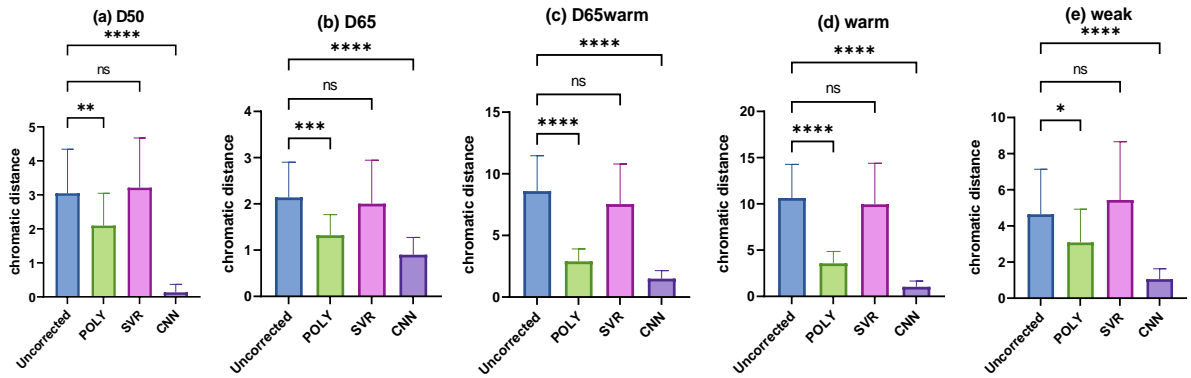
Fig. 5. ΔE_{mean} **of 24 color patches under five different lighting conditions. From left to right: D50, D65, D65warm, warm and weak. Black lines depict a significant difference between** ΔE_{mean} **of three methods and the uncorrected images**
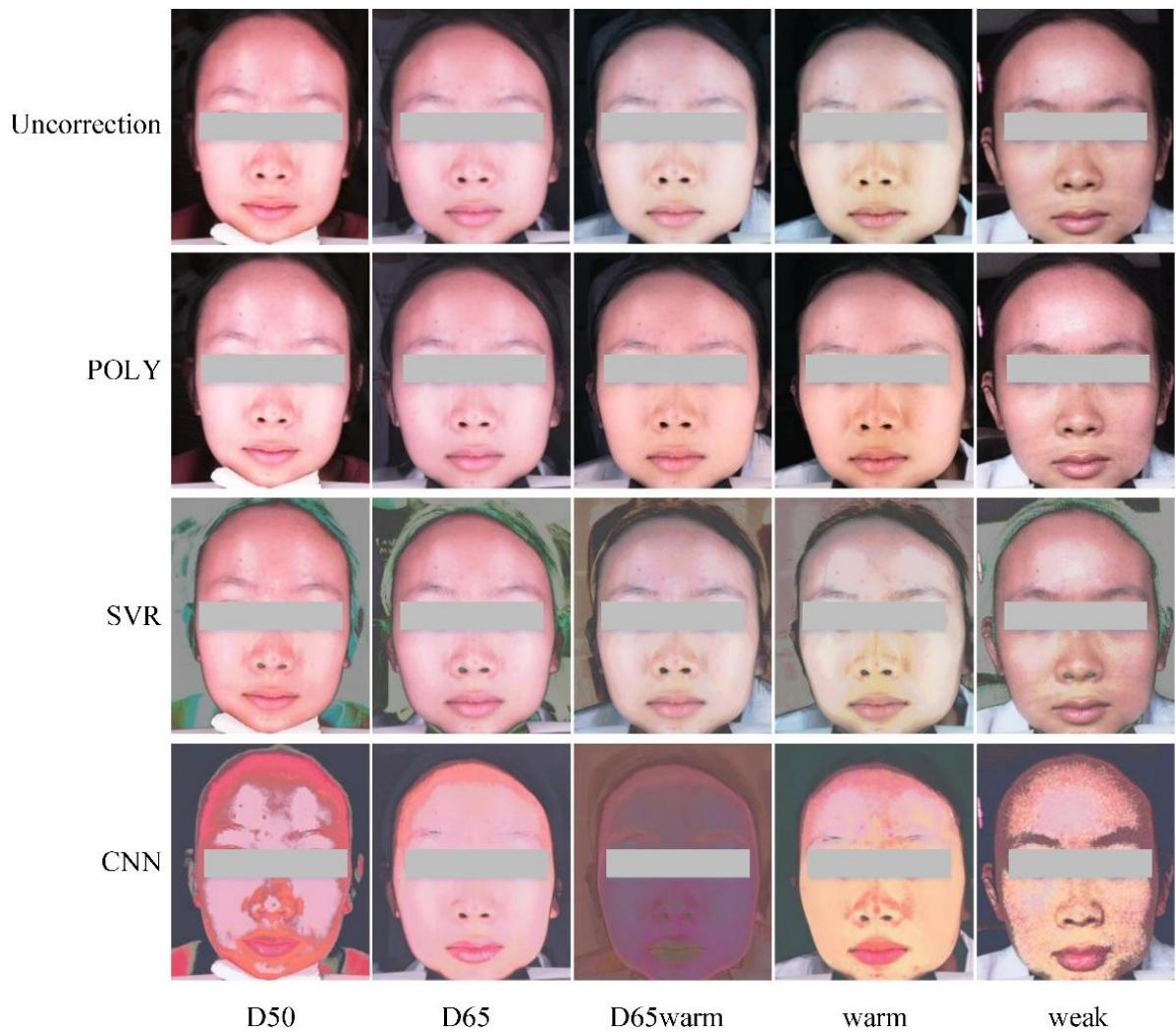

Fig. 6. Visual comparisons of three methods for facial color correction. From top to bottom: Uncorrected images, and corrected images by POLY, SVR, and CNN, respectively

3.2.3 Results of color correction algorithm selection

We compared the proposed method with the POLY-based correction method [3,19]. The comparative results of the objective evaluation are shown in Fig. 9. In the three methods, our proposed algorithm significantly outperforms other methods. Especially, the ΔE_{mean} of three methods in the weak illuminate environment have a significant difference. Fig. 8f showed that the ΔE_{mean} of our method under D50 and weak did not have a significant difference with that of D65. Moreover, the ΔE of our method under five different lighting conditions are lower than 3.0 (Fig. 9f), which shows that our method is suitable for facial image color correction task.

Meanwhile, Fig. 10 shows the qualitative performance of different color correction algorithms under five lighting conditions. From the subjective perception, before correction under warm and D65warm lighting conditions, the color tone of the facial image is yellowish. After correction, the color tone becomes ruddy, but the degree of ruddy by different algorithms varies. After correction by other algorithms, the facial image has the most reddish-dark tone under the weak lighting condition. The visual performance of our method is more consistent with the observed colors by human beings.
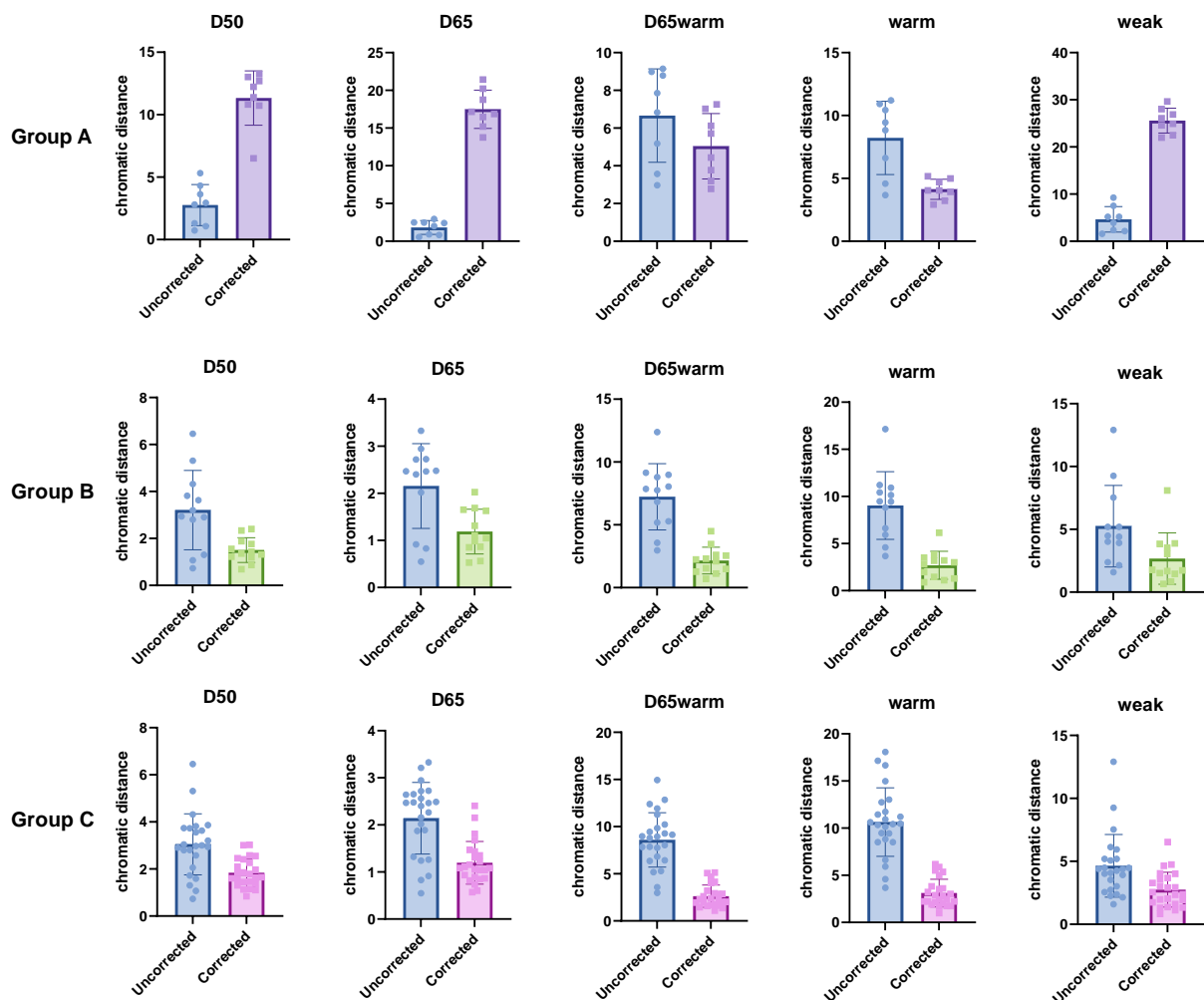

Fig. 7. ΔE_{mean} **of three groups under five different lighting conditions. From top to bottom: Groups A, B, and C, respectively. From left to right: D50, D65, D65warm, warm and weak. Different color discrete points present the chromaticity distances of each color patch in different groups**

3.2.4 Ablation studies with brightness adjustment

To further evaluate the effectiveness of our proposed method, we conducted ablation studies with brightness adjustment. The results are shown in Figs. 11 and 12. In addition, we applied brightness adjustment as preprocessing in Ref [3] and Ref [19]. From Fig. 11, we find that using only brightness adjustment did not satisfy the needs of color correction tasks. When we respectively appended the brightness adjustment operation to Ref [3] and Ref [19], the performance was slightly improved. Moreover, the objective analysis shows that the improvement is especially noticeable under the weak lighting condition.

Meanwhile, we can see that the facial images captured under the different lighting conditions have different highlight areas because these images suffered from the dynamic lighting variety. For example, in the fifth column of images in Fig. 12, the forehead area under the weak lighting condition has a highlight area. As the first step, the brightness adjustment produced a noticeable change in this area when we employed the brightness adjustment. Though the ΔE_{mean} of Ref [19] + brightness adjustment was reduced, the color tone of these facial images is still yellowish. Besides, the color tone of the facial image of Ref [19] + brightness adjustment is more reddish, especially the facial image captured under the D50 lighting condition. From the visual comparison, the corrected facial images of our method are visually better than those of other methods.
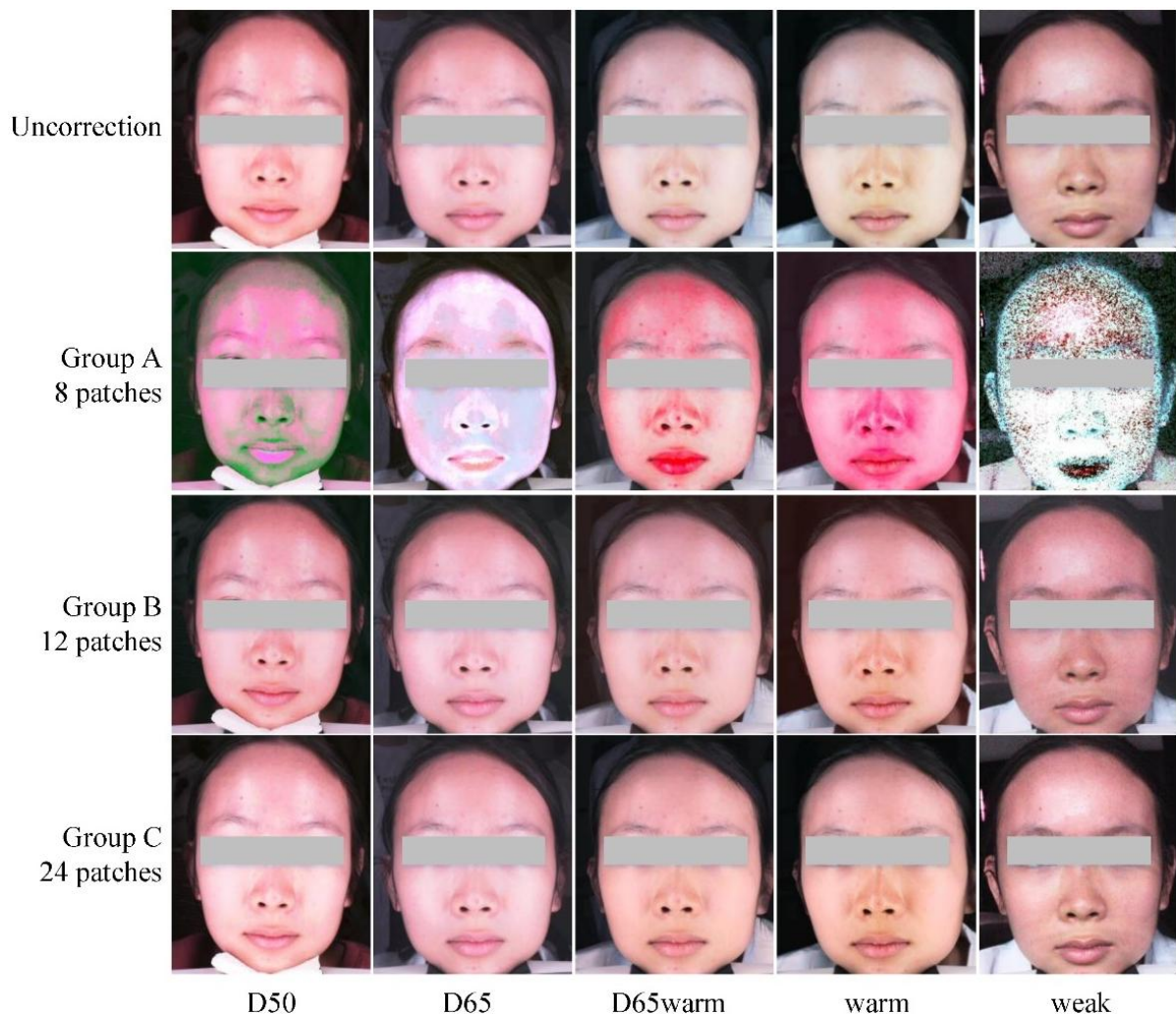

Fig. 8. Sample results of facial color correction on groups A, B, and C. From top to bottom: Groups A, B, and C, respectively. From left to right: D50, D65, D65warm, warm and weak
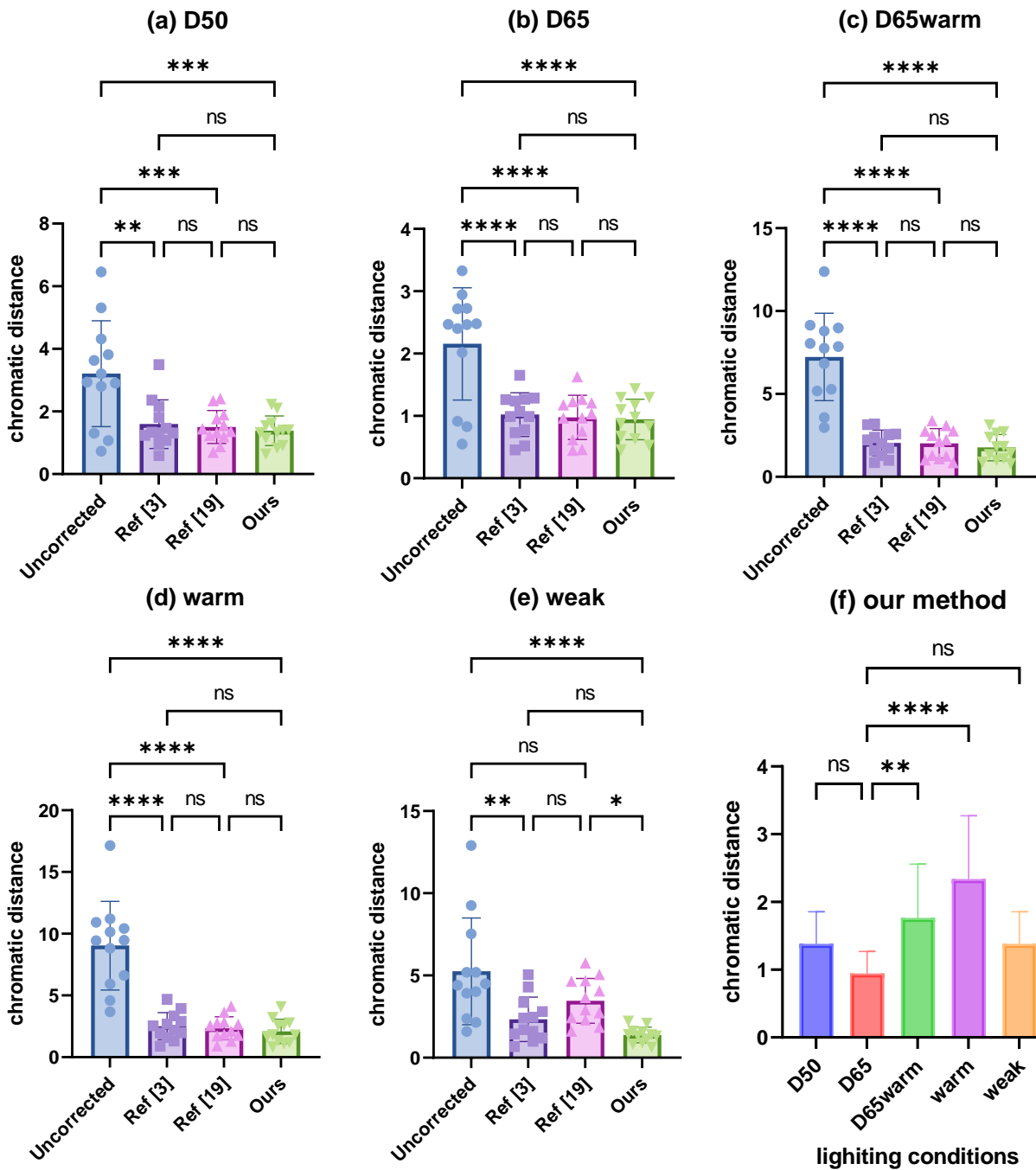
Fig. 9. ΔE_{mean} **of 12 color patches of three methods. (a)-(e)** ΔE_{mean} **of three methods under five different lighting conditions. (f)** ΔE_{mean} **of our method under five different lighting conditions**

3.3 DISCUSSION

In this section, we discuss the performance of the proposed color correction method compared to other methods under different lighting conditions. We proposed a two-stage color correction algorithm for facial images to obtain good perceptual adaptation.

With the excesses of deep learning in image processing [20,21], many scholars have used convolutional neural networks to obtain satisfactory performances. However, the preliminary work to train this network requires a lot of time and money to collect many images. For example, in Figs. 4 and 5, CNN can achieve good results in the chromatic distances, but it

cannot obtain a satisfactory subjective appearance. Therefore, we should analyze objective and subjective evaluation for the facial image color correction task. Additionally, SVR is a regression algorithm for small sample datasets, but it can be seen from Fig. 5 that the POLY is more suitable for this task.

In Figs. 9(a)-(e), these three methods' results differed significantly from those before correction. The ΔE_{mean} under five different lighting conditions are lower than 3.0. The objective evaluation indicated that the color checkers have the same visual perceptions after correction. Besides, we can see from Fig. 10 that the two-stage color correction model under weak lighting conditions has a better correction effect. There was a noticeable brightening change in the subject's forehead area. Therefore, our method is better than other POLY-based methods.

Previous methods for color correction of facial images have focused on single-stage algorithms. However, these methods ignore adjusting brightness under different lighting conditions. We utilized the adaptive white balance algorithm as the first step to adjust the brightness and then applied the ridge regression algorithm to optimize the color correction model (see Fig. S1). Due to facial shape features, the facial image contains forehead highlight areas and even different highlight areas under different lighting conditions.

Meanwhile, as seen in Fig. 8f, the chromaticity distances after correction in different illumination environments did not achieve consistency with those under the D65 condition. This difference may be caused by the illumination and color temperature of the environment.
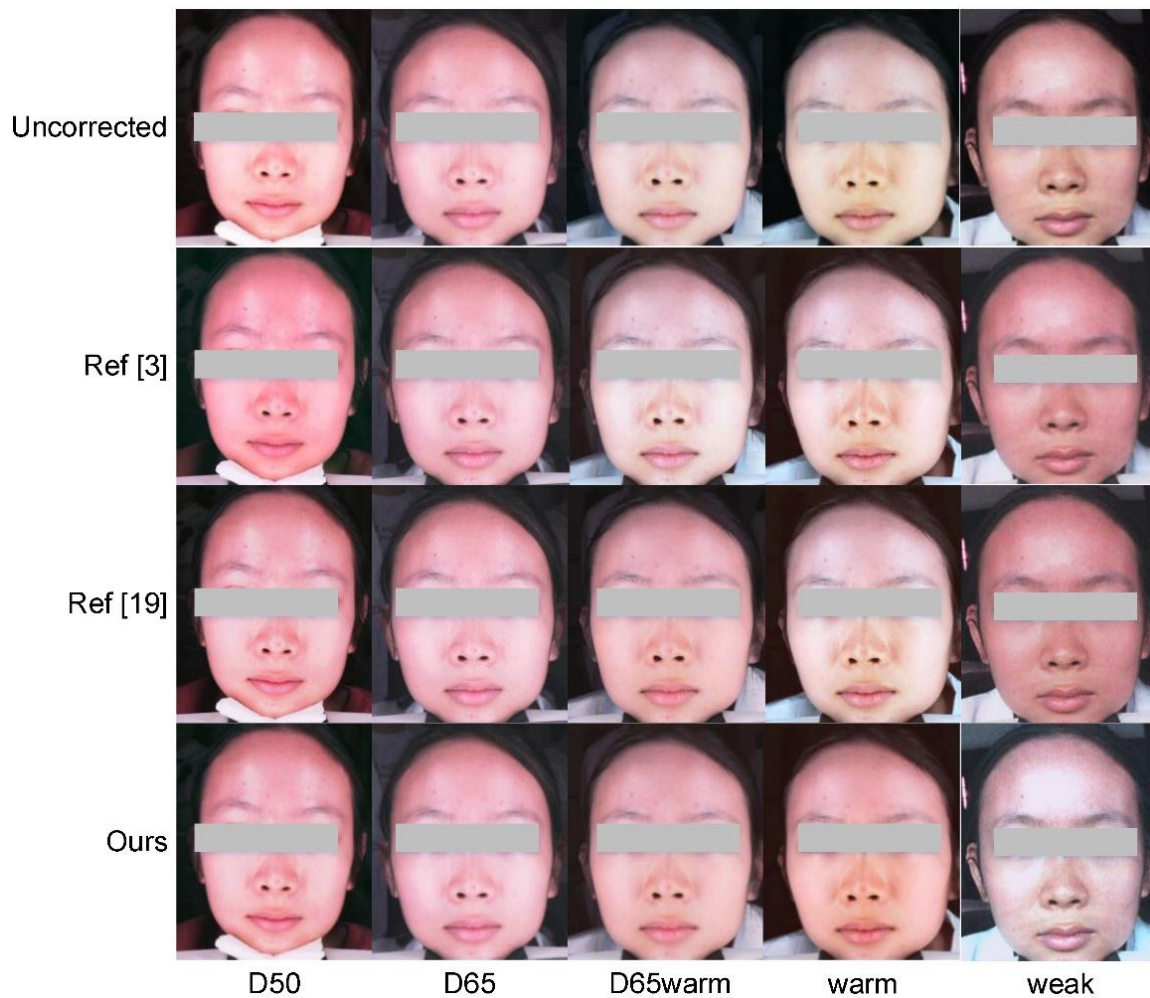

Fig. 10. Sample results of different color correction algorithms. From top to bottom: Uncorrected images, corrected images by Ref [3], Ref [19], and our method. From left to right: D50, D65, D65 warm, warm, and weak lighting conditions, respectively
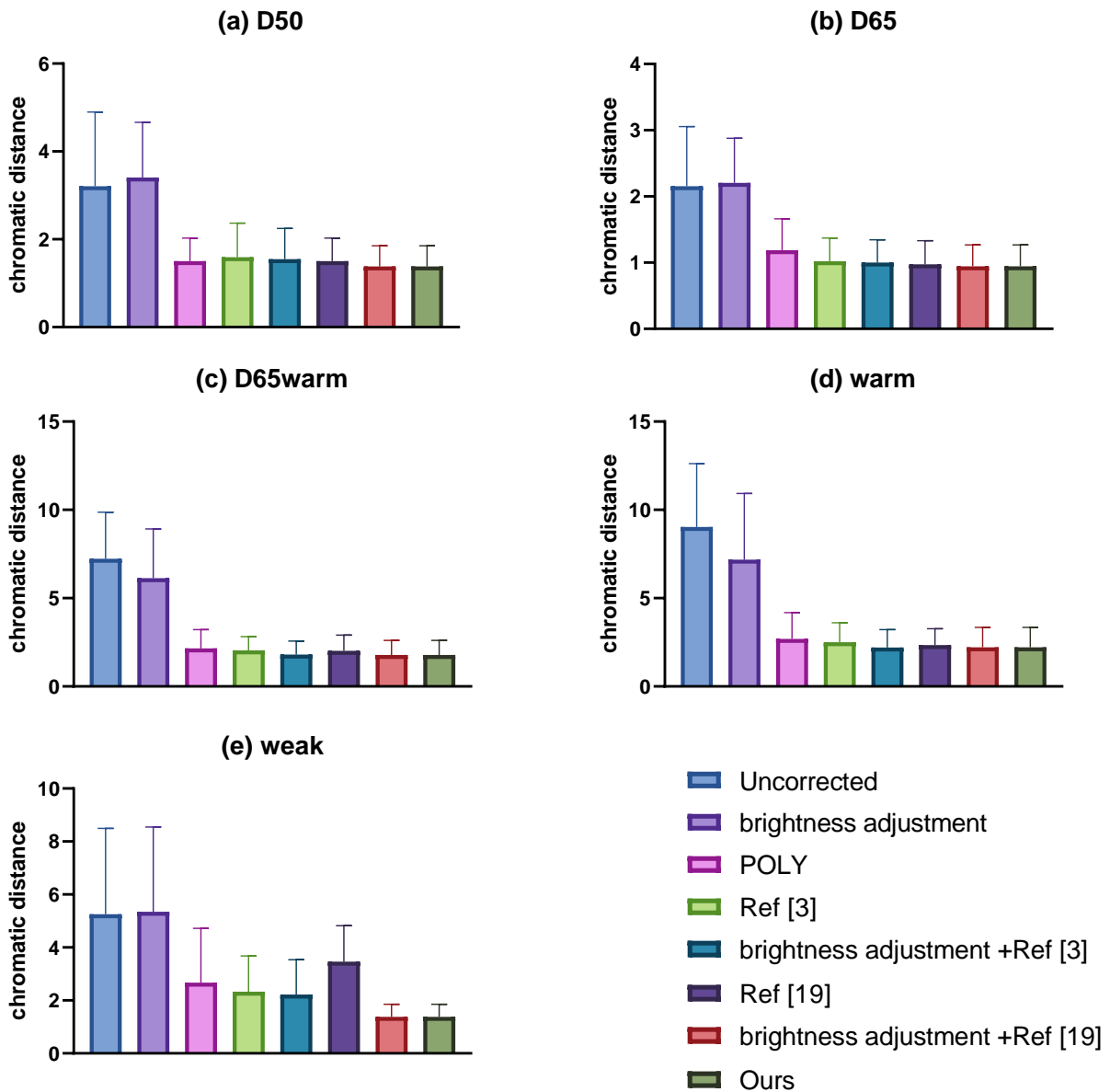
(a) D50

(b) D65

(c) D65warm

(d) warm

(e) weak

- Uncorrected
- brightness adjustment
- POLY
- Ref [3]
- brightness adjustment +Ref [3]
- Ref [19]
- brightness adjustment +Ref [19]
- Ours

Fig. 11. ΔE_{mean} **of seven methods under five different lighting conditions**

Besides, we selected 12 face-related color patches to optimize the color correction model. As shown in Fig. 6, the experimental results demonstrated that the ΔE_{mean} of Groups B and C performed very closely. Therefore, 12 facial-related color patches can perform the facial image color correction task, which is beneficial for reducing computational complexity and time.

Even though the proposed method has achieved good results under different lighting conditions, it still has some limitations [1]: The dataset only contains Asian, and the selected color patches mainly incline to Asian skin color [2]. Our model is designed for five lighting conditions. In recent years, the medical facial image captured in an open environment has become increasingly desirable for various medical diagnosis tasks.

In our future work, we aim to design a different race facial image color correction in an open environment. The dataset should contain more various skin colors. We hope more teams will explore this research direction, which is very important for clinical diagnosis.
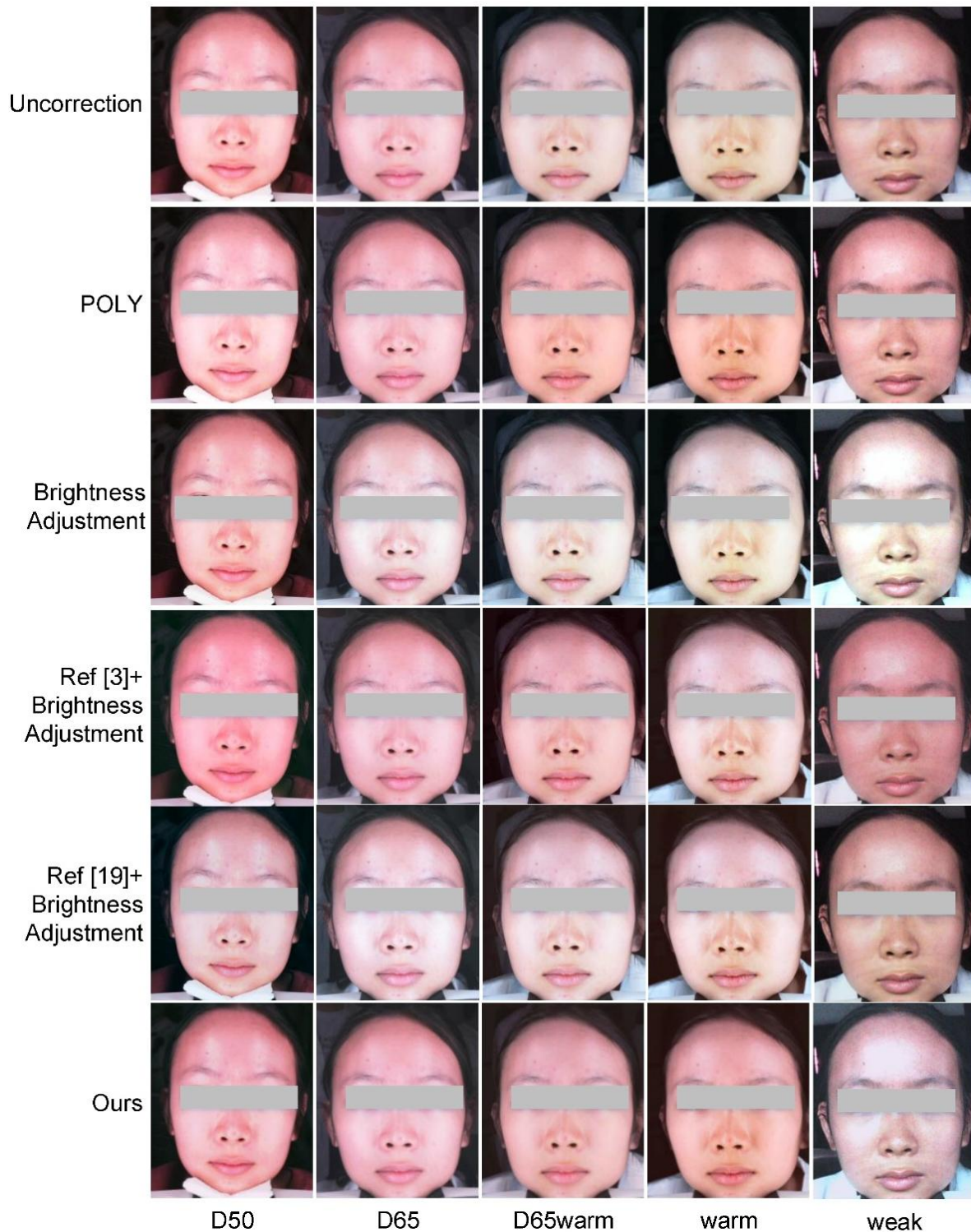
Fig. 12. Sample results of different color correction algorithms

4. CONCLUSION

This study proposed a two-stage color correction algorithm for the facial image. The experimental results show that 12 color patches for color correction of face distortion images are sufficient for this task. It is also further demonstrated that the regression model achieves more minor chromaticity differences in different lighting conditions. Moreover, we conducted the ablation

experiments for the white balance algorithm, and the experimental results show that the distance of chromaticity can be better reduced. However, some limitations must be noted. The proposed method must still be improved, considering the open environment for the facial color correction task.

Finally, our method is only to correct the facial images in the control environment, whose current form is not optimized for clinical practice. We need to make the algorithm better meet the need of real-world application devices. Furthermore, we should use face images from other teams for model validation while considering privacy protection security.

CONSENT

All authors declare that written informed consent was obtained from the patient for publication of this paper and accompanying amperages.

ETHICAL APPROVAL

All authors hereby declare that all experiments have been examined and approved by the appropriate ethics committee and have therefore been performed in accordance with the ethical standards laid down in the 1964 Declaration of Helsinki.

ACKNOWLEDGEMENT

COMPETING INTERESTS

Authors have declared that no competing interests exist.

REFERENCE

1. Niu JL, Zhao CB, Li GZ. A comprehensive study on color correction for medical facial images. Int J Mach Learn Cybern [Internet]. 2019;10(5):935–47. Available:http://dx.doi.org/10.1007/s13042-017-0773-6

2. Lu Y, Li X, Gong Z, Zhuo L, Zhang H. TDCCN: A two-phase deep color correction network for traditional Chinese medicine tongue images. Appl Sci. 2020;10(5):1–21.

3. Finlayson GD, Darrodi MM, Mackiewicz M. The alternating least squares technique for nonuniform intensity color correction. Color Res Appl. 2015;40(3):232–42.

4. Finlayson GD, Mackiewicz M, Hurlbert A. Color correction using root-polynomial regression. IEEE Trans Image Process. 2015;24(5):1460–70.

5. Zhang B, Wang X, Karray F, Yang Z, Zhang D. Computerized facial diagnosis using both color and texture features. Inf Sci (Ny) [Internet]. 2013;221:49–59. Available:http://dx.doi.org/10.1016/j.ins.2012.09.011

6. Zhuo L, Zhang P, Qu P, Peng Y, Zhang J, Li X. A K-PLSR-based color correction method for TCM tongue images under different illumination conditions. Neurocomputing. 2016;174(8):815–21.

7. Yang B, Chou HY, Yang TH. Color reproduction method by support vector regression for color computer vision. Optik (Stuttg) [Internet]. 2013;124(22):5649–56. Available:http://dx.doi.org/10.1016/j.ijleo.2013.04.036

8. Ding X, Jiang Y, Qin X, Chen Y, Zhang W, Qi L. Reading face, reading health: Exploring face reading technologies for everyday health. In: Conference on Human Factors in Computing Systems. 2019:1–13.

9. Zhuo L, Zhang J, Dong P, Zhao Y, Peng B. An SA-GA-BP neural network-based color correction algorithm for TCM tongue images. Neurocomputing [Internet]. 2014;134:111–6. Available:http://dx.doi.org/10.1016/j.neucom.2012.12.080

10. Zhang J, Yang Y, Zhang J. A MEC-BP-Adaboost neural network-based color correction algorithm for color image acquisition equipments. Optik (Stuttg) [Internet]. 2016;127(2):776–80.

11. Available:http://dx.doi.org/10.1016/j.ijleo.2015.10.120

12. Lixia M. Color correction of face image and its application in hepatopathy diagnosis. Harbin Institute of Technology; 2009.

13. Akazawa T, Kinoshita Y, Shiota S, Kiya H. Three-color balancing for color constancy correction. J Imaging. 2021;7(10).

14. Yan X, Wang G, Jiang G, Wang Y, Mi Z, Fu X. A natural-based fusion strategy for underwater image enhancement. Multimed Tools Appl. 2022;81(21):30051–68.

15. Huang H, Liao N, Zhao C, Fan Q. White balance conversion method of different camera based on triangle affine transform. Lect Notes Electr Eng. 2022;896:1–7.

16. Viola P, Jones M. Rapid object detection using a boosted cascade of simple features. In: Proceedings of the 2001 IEEE Computer Society Conference on Computer Vision and Pattern Recognition(CVPR 2001). 2001:511–8.

17. Zhang D, Zhang H, Zhang B. Tongue Image Analysis. Singapore:Springer; 2017.

18. Lam EY. Combining gray world and retinex theory for automatic white balance in digital photography. In: Proceedings of the Ninth International Symposium on Consumer Electronics, 2005 (ISCE 2005). 2005:134–9.

19. Lu Y, Li X, Zhuo L, Zhang J, Zhang H. Dccn: A deep-color correction network for traditional Chinese medicine tongue images. 2018 IEEE Int Conf Multimed Expo Work ICMEW 2018. 2018;1–6.

20. Su Q, Cheng H, Sun W, Zhang F. A novel correction algorithm based on polynomial and TPS models. In: International Conference of Information Technology, Computer Engineering and Management Sciences. 2011:52–5.

21. Çalişkan A. classification of tympanic membrane images based on VGG16 model. Kocaeli J Sci Eng. 2022;5(1):105–11.

22. Çalişkan A. A new approach for congestive heart failure and arrhythmia classification using downsampling local binary patterns with LSTM. Turkish J Electr Eng Comput Sci. 2022;30(6):2145–64.
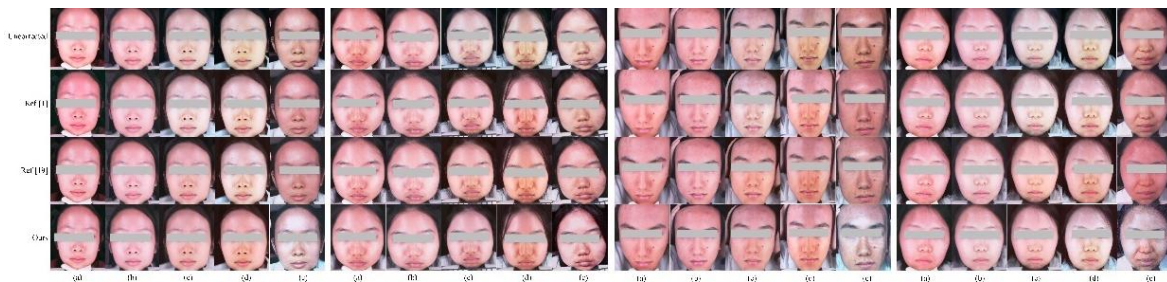
APPENDIX

Fig. S1. Sample results of different color correction algorithms. From top to bottom: Uncorrected images, corrected images by Ref (3), corrected images by Ref (19), and corrected images by our method. From left to right: (a) D50, (b) D65, (c) D65 warm, (d) warm, and (e) weak lighting conditions, respectively